

# Properties of phenol-removal aerobic granules during normal operation and shock loading

He-Long Jiang · Abdul Majid Maszenan ·  
Zhi-Wei Zhao · Joo-Hwa Tay

Received: 28 August 2009 / Accepted: 3 November 2009 / Published online: 27 November 2009  
© Society for Industrial Microbiology 2009

**Abstract** The physical structure and activity of aerobic granules, and the succession of bacterial community within aerobic granules under constant operational conditions and shock loading were investigated in one sequencing batch reactor over ten months. While the maturation phase of the granulation process began on day 30, the structure of microbial community changed markedly until after three months of reactor operation under constant conditions with a loading rate of 1.5 g phenol L<sup>-1</sup> day<sup>-1</sup>. A shock loading of 6.0 g phenol L<sup>-1</sup> day<sup>-1</sup> from days 182–192 led to divergence of bacterial community, an inhibition of the biomass activity, and a decrease in phenol removal rate in the reactor. However, phenol was still completely removed under this disturbance. After the shock loading, the mean sizes of aerobic granules increased, and the activity of the microbial population within the granules decreased, although there appeared highly resilient for the dominant bacterial community of aerobic granules which mainly included  $\beta$ -Proteobacteria. Correlation analysis suggested

that biomass concentration and biomass loading were significantly related to the community composition of aerobic granules during the whole operational period. The development of a relatively stable bacterial community in aerobic granules implied that those distinct dominant microbes in aerobic granules were favorably selected and proliferated under the operational conditions.

**Keywords** Aerobic Granules · Microbial Community · Phenol Biodegradation · Shock Loading · Stability

## Introduction

The development and application of aerobic granules in sequencing batch reactors (SBRs) for biological wastewater treatment has attracted increasing interests [4]. Like their anaerobic counterparts, aerobic granules are dense spherical self-immobilized aggregates of microorganisms with a strong compact structure and excellent settling ability. The compact structure of aerobic granules provides spatial heterogeneity which led to niche differentiation within aerobic granules and increased physiological diversity in the resident microbial community [15]. Laboratory studies have indicated that aerobic granule-based bioreactors possesses the high biodegradation capacity for toxic and recalcitrant compounds [1, 23, 27, 29] as well as simultaneous chemical oxygen demand (COD) and nutrients removal [6, 8, 16]. Although the organic loading rate is typically utilized to investigate granule formation and structural stability [2, 7], the stability of aerobic granule-based bioreactors under shock loading was not studied in detail. In fact, biological treatment processes may be exposed to unexpected short-term toxic pollutant loadings when applied practically.

**Electronic supplementary material** The online version of this article (doi:10.1007/s10295-009-0668-y) contains supplementary material, which is available to authorized users.

H.-L. Jiang (✉)  
State Key Laboratory of Lake Science and Environment,  
Nanjing Institute of Geography and Limnology,  
Chinese Academy of Science, 73 East Beijing Road,  
Nanjing 210008, People's Republic of China  
e-mail: hljiang@niglas.ac.cn

H.-L. Jiang · A. M. Maszenan · J.-H. Tay  
School of Civil and Environmental Engineering,  
Nanyang Technological University, Singapore, Singapore

Z.-W. Zhao  
College of Electronic Science and Technology, Southeast  
University, Nanjing, People's Republic of China

Phenol is a commonly found toxic waste byproduct in many industries. While phenol removal has been carried out for many years by activated sludge systems, the increment in phenol loads from 1.0 to 1.5 g phenol L<sup>-1</sup> day<sup>-1</sup> has been reported to cause the breakdown of activated sludge processes because of the toxicity exerted by high concentrations of phenol [28]. The fluctuation in substrate loading also influenced the composition of the microbial community in the biological treatment system. The population shift in microbial community was regarded as one of the causes of the breakdown of those treatment processes [9, 28].

Therefore, the careful analysis of the microbial community succession under constant and disturbance operational conditions could obtain clues to improvement in the design and operation of biological treatment systems. Fingerprinting pattern analysis such as polymerase chain reaction-denaturing gradient gel electrophoresis (PCR-DGGE), based on 16S rRNA gene sequences, is widely applied to detect shift in microbial community over time under different environmental conditions [22]. These fingerprinting patterns can be statistically analyzed to interpret the relationship between functional stability and microbial community dynamics [10].

In this study, one SBR was operated for ten months with aerobic granules formed during the initial three weeks of operation. After both reactor performance and granule properties reached to a steady state, the reactor was subjected to a 10-day shock loading and was continuously run under normal condition until the reactor returned to steady state again. The microbial community in aerobic granules was characterized with DGGE. The overall objectives of this study were to investigate the change of physical structure and activity of aerobic granules after shock loading, and the succession of bacterial community in aerobic granules.

## Materials and methods

### Reactor operation

One column-type SBR with a diameter 5 cm and a height of 102 cm was operated at 25°C. The working volume of the reactor was 2.0 L. The sequentially operational cycle time in the reactor was 4 h with 15 min of filling, 15 min of effluent withdrawal, 10 min of settling time, and 200 min of reaction period. Fine air bubbles were introduced at an air flow rate of 1.0 L min<sup>-1</sup> through a dispenser located at the bottom of the reactor. The sequential operation of the reactor was automatically controlled by timers, while two peristaltic pumps were employed for influent filling and effluent withdrawal respectively.

Effluent was discharged 51 cm above the reactor bottom at a volumetric exchange ratio of 50%. The pH was maintained at 6.7 ± 0.2 with the addition of phosphate buffer in the influent.

The reactor was fed with phenol as sole organic carbon source by using a synthetic wastewater. At a influent phenol concentration of 0.5 g L<sup>-1</sup>, the concentrations of NH<sub>4</sub>Cl, MgSO<sub>4</sub>·7H<sub>2</sub>O, K<sub>2</sub>HPO<sub>4</sub>, and KH<sub>2</sub>PO<sub>4</sub> were 0.2, 0.13, 1.65, and 1.35 g L<sup>-1</sup>, respectively. Under the variance of influent phenol concentrations, the concentrations of those minerals changed with a same ratio. The media was supplemented with 1 ml L<sup>-1</sup> of micronutrients, as described by Beun et al. [4]. The reactor was inoculated with activated sludge taken from a municipal wastewater treatment plant leading to a final concentration of about 2.0 g suspended solid (SS) L<sup>-1</sup>. The whole operation lasted about ten months, and was divided into three phase. In Phase I, a volumetric loading of 1.5 g phenol L<sup>-1</sup> day<sup>-1</sup> with an influent phenol concentration of 0.5 g L<sup>-1</sup> was maintained until day 182. In Phase II, the reactor was subject to a shock loading of 6.0 g phenol L<sup>-1</sup> day<sup>-1</sup> by increasing the influent phenol concentration to 2.0 g L<sup>-1</sup> from days 182 to 192. In Phase III with time duration of four months, the loading returned to 1.5 g phenol L<sup>-1</sup> day<sup>-1</sup> by decreasing the influent phenol concentration to 0.5 g L<sup>-1</sup> after day 192.

### DNA extraction and denaturing gradient gel electrophoresis (DGGE)

Biomass samples for nucleic acid extraction were taken out from the reactor and maintained on ice until centrifugation. Collected samples were centrifuged (10,000 g, 20 min) in 4°C and washed once with 10 mM RNase-free Tris buffer (pH 7.8). The pellet was immediately frozen in liquid nitrogen and stored at -20°C until analysis. Genomic DNA of biomass samples in the reactor was extracted using the bead beating method [15]. For DGGE analysis, PCR primers P2 and P3 with 40 bases of GC clamp were used to amplify the V3 region of bacterial 16S rRNA gene [22]. After electrophoresis the gel was stained with ethidium bromide for 30 min, and viewed and photographed with an EDAS 290 gel imaging system (Kodak, USA). Selected bands were excised to perform PCR to obtain 16S rRNA nucleotide sequencing. The partial sequences were assembled using BioEdit software, and have been deposited in the NCBI nucleotide sequence databases under accession nos. EF429317 to EF429326.

### DGGE gel analysis

The image files for the different gels were pasted together in one file with tag image file format, followed by conversion

and normalization using GelCompar 4.0 software package (Applied Maths, Kortrijk, Belgium). To aid in the conversion and normalization of gels, a marker consisting of seven clones was added on the outsides of the gels as external references. In addition, bands in DGGE gels which appeared in most of the lanes were used as internal references for facilitating conversion and normalization of gel images. In band assignment, bands with densities (based on peak areas) smaller than 2% of the maximum single-band density in one lane were firstly discarded, and then a 1% band position tolerance (relative to the total length of the gel) was applied, which indicates the maximal shift allowed for two bands in different DGGE lanes to be considered as identical. Band pattern similarities were calculated with the Dice coefficient based on the band presence/absence by the unweighted pair group clustering method with arithmetic averages (UPGMA), and displayed graphically as dendrogram. Band presence or absence in DGGE lanes was scored as 1 or 0, respectively. These 1/0 numbers were also exported to the spreadsheet program Excel for principal components analysis (PCA) and correspondence analysis (CA) using the software GenStat for Window 8th edition (VSN International Ltd, Herts, UK). To interpret relationship between community structure and reactor performance, the first three principal components calculated from DGGE profiles were used as the dependent  $y$ -variable, and reactor operation parameters were used as the predictors ( $x$ -variable) in regression analysis.

Relative band densities calculated by the software GelCompar were also used for determining the Shannon diversity index (SDI). Because the DGGE banding pattern reflects the most abundant rDNA types of the microbial community, the diversity index calculated from the DGGE profile is a relative term but still applicable to monitoring a whole range of changes in community structure [9]. The SDI was calculated with each band corresponding to a single species, and that band density was equivalent to species abundance [9], as shown in following equation:  $SDI = -\sum p_i \log p_i$ , where  $p_i$  is the proportion of the community that is made up of species  $i$  (density of band  $i$ /total density of all bands in the lane). The equitability index (EI), an indication of the evenness of species distribution, was determined according to the following equation:  $EI = SDI/\log n$ , where  $n$  is the total number of bands in the lane.

#### Analytical methods

Biomass size was measured by an image analysis system (Quantimet 500 image analyzer, Leica Cambridge Instruments, Cambridge, UK). Suspended solid (SS), volatile suspended solid (VSS), sludge volume index (SVI) after 30 min of settling, specific oxygen utilization rate (SOUR),

and phenol concentrations were measured as described previously [14]. Soluble total organic carbon (TOC) was measured with a TOC analyzer (TOC-Vcsh, Shimadzu, Kyoto, Japan). Mean cell retention time (MCRT) was calculated by dividing biomass content in the reactor by the biomass discharged in one day.

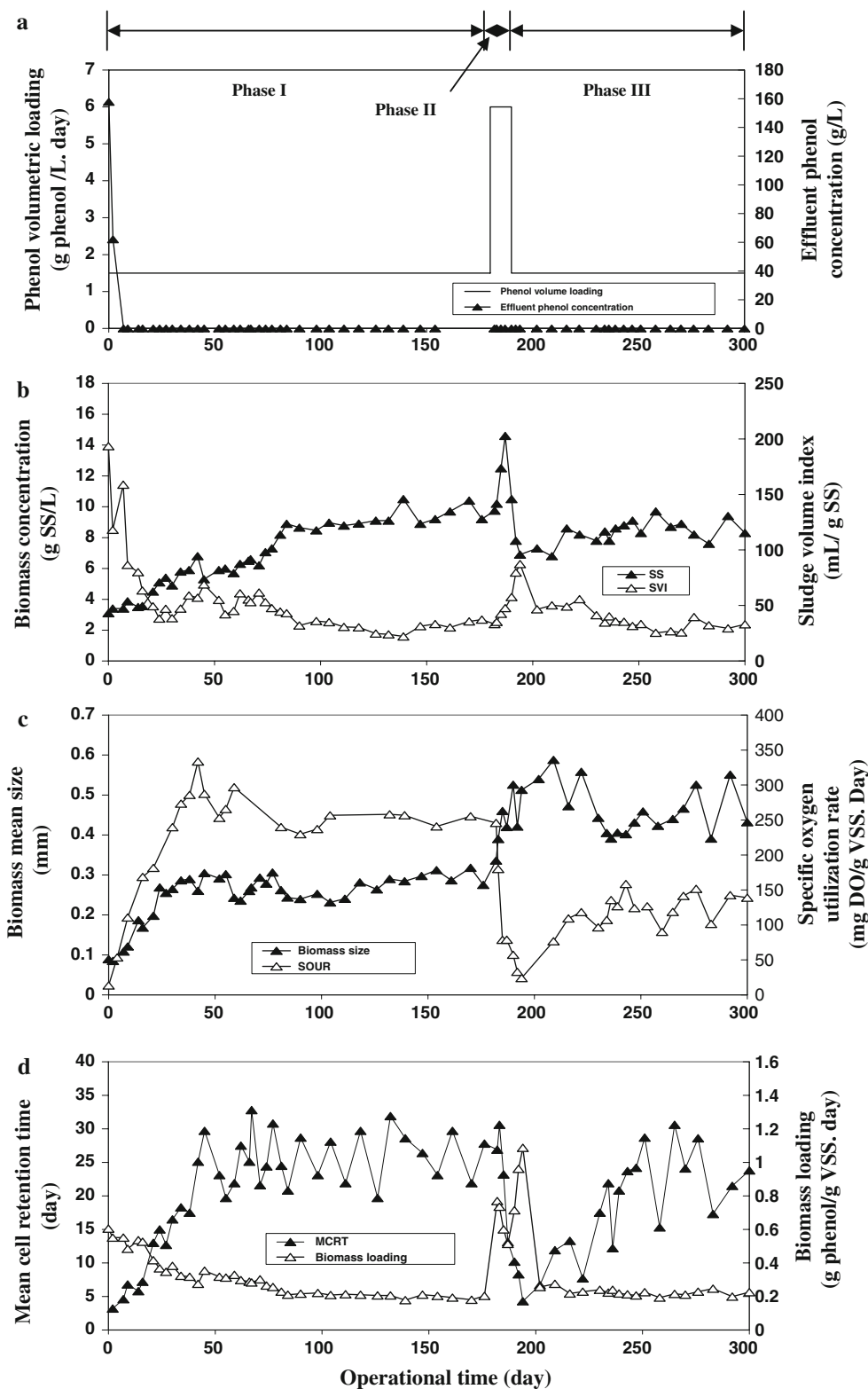
## Results

### Reactor performance and effect of shock loading

The reactor was inoculated with activated sludge and operated for ten months with phenol as sole organic carbon source. While a volumetric loading rate of 1.5 g phenol  $L^{-1} day^{-1}$  was applied in the Phases I and III, a shock loading of 6.0 g phenol  $L^{-1} day^{-1}$  was used in Phase II. Except during the initial seven days, phenol could not be detected in the effluent during the whole operational period. As a result of a short settling time of 10 min, aerobic granulation took place during the first three weeks leading to a mean biomass size of about 0.2 mm (Fig. 1c). Thereafter, biomass sizes remained within the range 0.2–0.3 mm in Phase I. Accompanied with granule formation, biomass concentration, biomass settleability, biomass activity, and MCRT gradually increased. After the formation of granules, the amount of suspended biomass was less than 3% of the total biomass in the reactor. The biomass settleability was reflected by the parameter SVI, and the low SVI value represents high settleability. Compared to an initial SVI value of 120 mL  $g SS^{-1}$ , biomass SVI values decreased to 30 mL  $g SS^{-1}$  on day 32. From days 91 to 182, these parameters (biomass concentration, biomass settleability, biomass activity, and MCRT) were considered to be stable. During this period, the average values for biomass concentrations and biomass activity were  $9.7 \pm 0.6 g SS L^{-1}$  and  $251.4 \pm 15.3 mg$  dissolved oxygen (DO)  $g VSS^{-1} day^{-1}$ , respectively.

When the reactor was subjected to a shock loading from days 182–192 in Phase II, biomass concentrations initially showed a sharp increase to 14.7  $SS L^{-1}$  on day 187, followed by a sharp decline to 7.8  $SS L^{-1}$  on day 192 (Fig. 1b). The decline of biomass concentration was directly related to the decrease in biomass settleability. While the biomass loading was only 0.22 g phenol  $g^{-1} VSS day^{-1}$  prior to the shock loading, the biomass loading increased to 1.09 g phenol  $g VSS^{-1} day^{-1}$  after ten days of shock loading (Fig. 1d). Accompanied with this disturbance, MCRT also decreased from 26.1 to 4.3 days. Although the shock loading did not disintegrate aerobic granules, it did lead to decrease in biomass settleability and increase in biomass size. At the same time, biomass activity sharply decreased to 24.1 mg DO  $g VSS^{-1} day^{-1}$ .

**Fig. 1** Reactor operation parameters and performance. Phenol volumetric loading and effluent phenol concentration (a) Biomass concentration and sludge volume index (b) Biomass mean size and specific oxygen utilization rate (c) Mean cell retention time and biomass loading (d)



In Phase III, the shock loading stopped, and the reactor was continuously operated for about four months with operation conditions same as those in Phase I. It was found that biomass concentration, biomass settleability, biomass

loading, and MCRT gradually returned to the levels prior to the shock loading. However, the values of biomass size and biomass activity at the end of Phase III were significantly different from those at the end of Phase I ( $p < 0.01$ )

**Table 1** Characteristics of reactor performance and aerobic granules during the end periods of phases I and III

	End period of phase I	End period of phase III	Significant coefficients ( <i>P</i> ) of difference between mean values at the ends of phases I and III <sup>a</sup>
Biomass concentration in the reactor (g SS L <sup>-1</sup> )	9.7 ± 0.6	8.5 ± 1.1	0.080
Total organic carbon removal efficiency (%)	98.0 ± 0.6	97.9 ± 0.4	0.765
Phenol removal efficiency (%)	99.9%	99.9%	0.164
F/M ratio or biomass loading (g phenol g SS <sup>-1</sup> day <sup>-1</sup> )	0.20 ± 0.02	0.22 ± 0.03	0.254
Mean cell residence time (days)	32.9 ± 3.1	29.5 ± 5.2	0.274
<b>Mean biomass size (mm)</b>	<b>0.31 ± 0.04</b>	<b>0.48 ± 0.09</b>	<b>0.007</b>
Sludge volume index (mL g SS <sup>-1</sup> )	34.1 ± 4.2	32.0 ± 6.9	0.60
<b>Specific oxygen utilization rate (mg DO g VSS<sup>-1</sup> day<sup>-1</sup>)</b>	<b>251.4 ± 15.3</b>	<b>135.2 ± 27.1</b>	<b>0.0002</b>

<sup>a</sup> Significant coefficients were calculated using the student's *t*-test at the 95% confidence level. Significant coefficients less than 0.01 were printed in bold

at the 95% confidence level) (Table 1). Compared to the values at the end of Phase I, biomass sizes increased to 0.48 ± 0.09 mm and biomass activity decreased to 135.2 ± 27.1 mg DO g VSS<sup>-1</sup> day<sup>-1</sup> at the end of Phase III. In fact, image analysis also suggested the change in the physical structure of aerobic granules (Fig. S-1, supporting information). Besides small granules in the reactor, there existed big granules with a diameter of 1-1.5 mm at the end of Phase III.

Phenol and TOC concentrations were measured during one cycle in the reactor at the ends of the three phases (Fig. 2). The time zero coincided with the start of aeration in one cycle. Because the volumetric exchange ratio for the reactor was 50% and effluent phenol and TOC concentrations were insignificant compared to influent phenol and TOC concentrations, the phenol and TOC concentrations in the reactor at time zero were approximately one-half of the influent phenol and TOC concentrations. Through linear regression analysis, the phenol removal rates at the ends of Phases I and III were almost same with a value of 0.47 g phenol L<sup>-1</sup> h<sup>-1</sup>, and higher than that at the end of Phase II. The phenol removal rate at the end of Phase II was only 0.33 g phenol L<sup>-1</sup> h<sup>-1</sup>. The lower phenol removal rate at the end of Phase II corresponded to the low activity of biomass. Phenol concentrations were higher than TOC concentrations during the initial part of the cycles. The difference in concentration was expected, given the carbon content and molecular weight of phenol. While only 30 min were required for complete removal of phenol and TOC at the ends of Phases I and III, it took nearly 3 h for complete removal at the end of Phase II.

**Bacterial community succession**

The bacterial population succession with reactor operation was detected by isolating DNA from biomass samples taken from different periods, and then performing DGGE

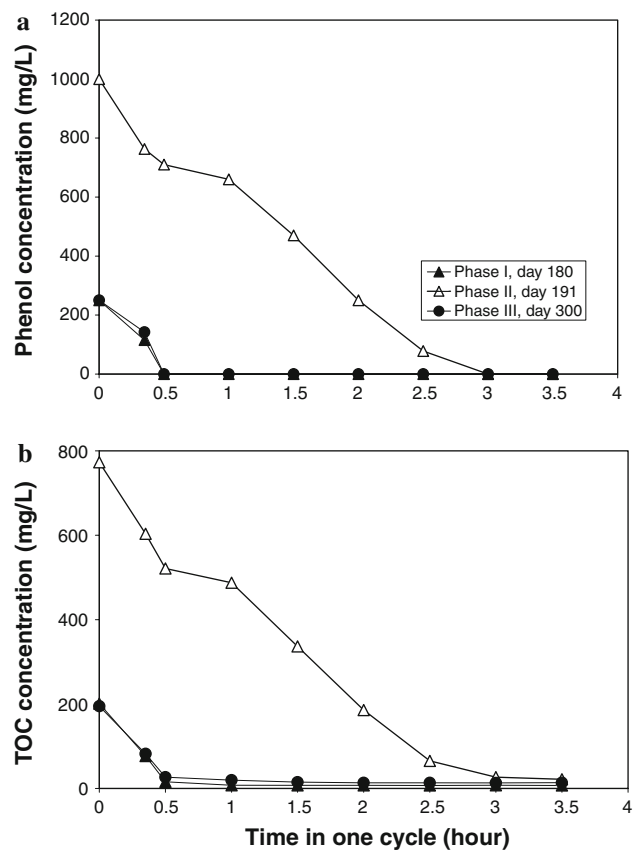


**Fig. 2** Profiles of phenol removal (a) and TOC removal (b) in one cycle at the ends of three Phases

analysis of amplified 16S rRNA gene fragments in four gels (Fig. 3). The methodological reproducibility of DGGE profiles was firstly tested through separate DNA extraction and PCR reactions from the same biomass samples. It was demonstrated 97-100% similarity of DGGE bands based on presence or absence for replicate samples. The DGGE patterns for the biomass samples appeared dynamic during the initial three months and then became similar, indicating

a relatively stable microbial community. Dominant DGGE bands in the lane at the end of the experiment were excised for DNA sequencing. Recovered bands were reamplified by PCR and run on a DGGE gel to confirm purity. This was repeated several times to obtain a pure DNA product for sequencing. Partial 16S rRNA gene sequences of close to 200 nucleotides were successfully obtained from ten different DGGE bands (B01–B10 in Fig. 3) and compared with nucleotide sequences from GenBank. All of the band sequences grouped with member of Proteobacteria (Table S-1, supporting information). With one and two sequences in the  $\gamma$  and  $\alpha$  subdivisions, the remaining seven clustered with the  $\beta$  subdivision.

For statistics analysis of microbial community, DGGE gels were converted and normalized. The difference among these lanes in DGGE gels were reflected using the Dice coefficient and UPGMA, based on a similarity matrix calculated from the presence/absence of DGGE bands (see Fig. S-2, supporting information). To see whether the interpretation of DGGE data varied with applied statistics methods, DGGE gels were also analyzed using multivariate ordination methods. Both PCA and CA produced a graphical representation of samples along two or more axes of reference (dimensions) that contain a fraction of the total variability. Samples with similar community structures were closer together in the multidimensional plot. The amount of data scatter in the multidimensional plot represents the variability of the community. PCA of the DGGE band profiles corresponded to cluster analysis by UPGMA, but provided clear information about microbial community succession

with reactor operation (Fig. 4a). PCA revealed that the majority of the change occurred during the days 0–91, while from days 111–300 the points tended to cluster together, confirming that the community structures were similar during this lengthy period. Only on day 185, the microbial community in the reactor had diverged greatly from Group II, suggesting fluctuation of the microbial composition during the period from days 183–187. However, this point was not reflected by CA (Fig. 4b), which may be due to different computation models used. Although results from CA were not all identical to those from PCA, initial dynamic and late relative stability of microbial community was still reflected by CA. So, all these three statistics methods gave an almost consistent and reproducible interpretation of DGGE profiles.

#### Correlation analysis of principal components with reactor operation variables

The first three principal components variables were chosen for exploration of the link between bacterial community composition and reactor operation parameters by correlation analysis, as shown in Table 2. The principal components 1–3 explained 33.7, 18.9 and 10.5% of the variance, respectively. While biomass concentration and biomass loading were significantly related to the principal component (PC) 1, biomass size, SVI, MCRT, and SOUR were significantly related to the PC 2. Among those correlation coefficients, the correlation coefficient between SOUR and PC 2 had the highest value ( $R = 0.828$ ,  $P < 0.001$ ).

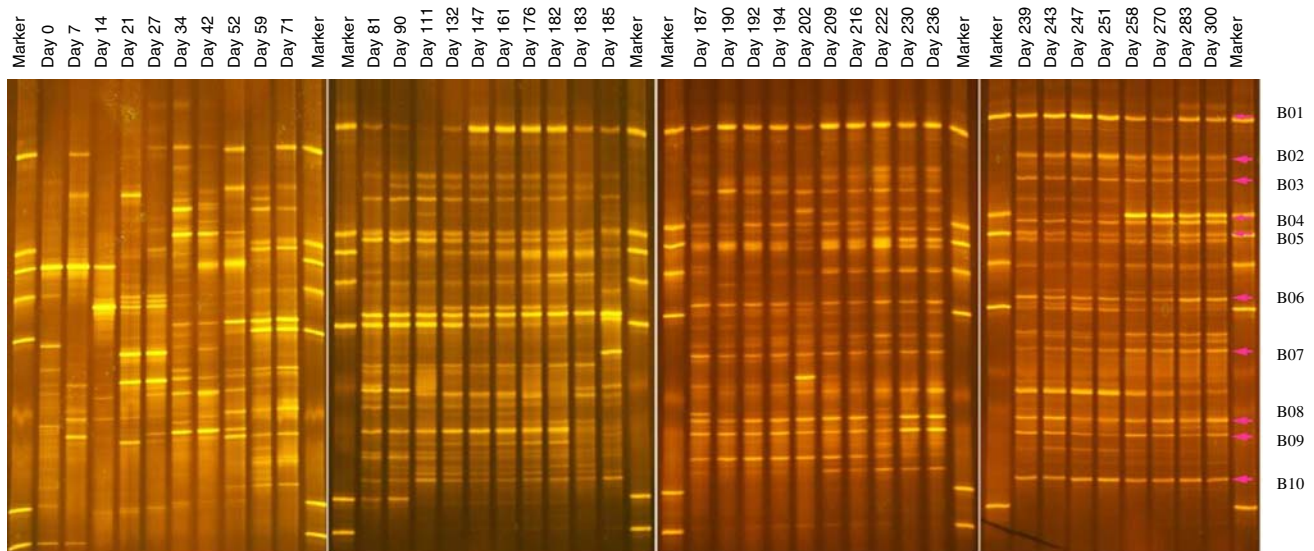


**Fig. 3** An ethidium bromide-stained 10% polyacrylamide denaturing gradient gel (30–70%) with DGGE profiles of 16S rDNA gene fragments after PCR amplification of nucleic acids from biomass taken from the reactor. The source of each fingerprint is indicated above each lane

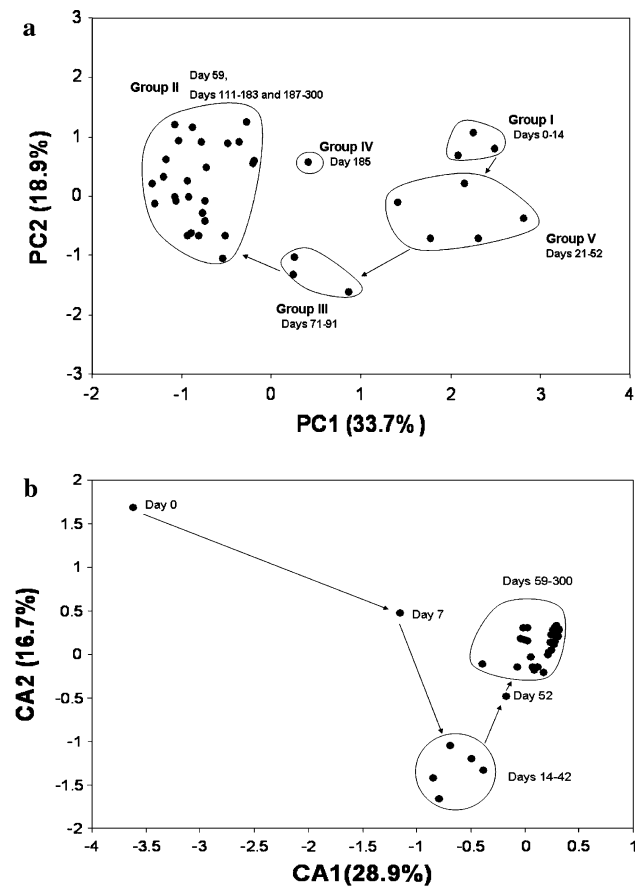


**Fig. 4** Two-dimensional plots of principal component analysis (PCA) (a) and correspondence analysis (CA) (b) for the DGGE gels

**Bacterial community diversity**

The SDI and EI values based on DGGE profiles were calculated and shown in Fig. 5. SDI values decreased from 1.05 to 0.48 in the initial 14 day, suggesting a decrease in bacterial diversity during this period. Thereafter SDI values increased and stabilized with a mean value of 1.18. The

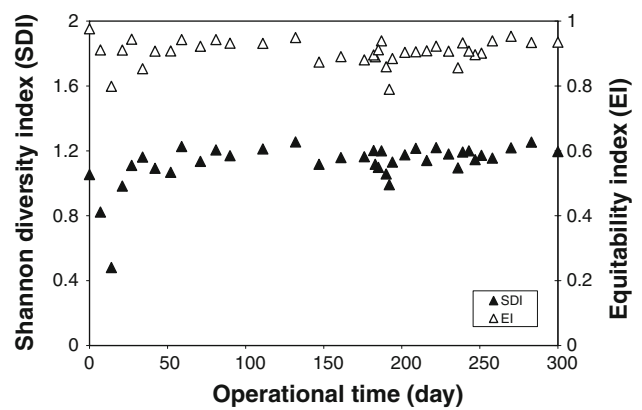


**Fig. 5** Shannon diversity index (SDI) and equitability index (EI) of microbial community with reactor operation

parameter EI reflects the evenness of species distribution. EI values did not show much variance with a mean value of 0.91 during the whole operational period.

**Discussion**

This study demonstrated that bacterial communities in the aerobic granules- developed bioreactor were dynamic during the initial three months, and then converged to the relatively stable stage during the next seven months except during the shock loading. The shock loading led to divergence of bacterial community during the period of days 183-187. According to observation of cell aggregate growth, aerobic granulation as a successional process was categorized into four phase: acclimating, shaping, developing and maturation [25]. The matured phase was characterized by almost constant size and settleability of aerobic granules. In this study, the maturation phase of the granulation process could be considered to begin on day 30. After that, granule size and settleability remained relatively stable until shock loading. This meant that there

**Table 2** Correlation coefficients (*R*) and their significance (*P*) between the first three principal components (PC) from DGGE band analysis of *Bacteria* 16S rDNA gene fragments and reactor operation parameters

	PC1		PC2		PC3	
	<i>R</i>	<i>P</i>	<i>R</i>	<i>P</i>	<i>R</i>	<i>P</i>
Biomass concentration	<b>-0.591</b>	<0.0001	0.022	0.448	0.266	0.054
SVI <sup>a</sup>	0.251	0.065	<b>0.381</b>	0.0091	-0.196	0.119
MCRT <sup>b</sup>	-0.359	0.013	<b>-0.581</b>	<0.0001	0.026	0.437
Biomass loading	<b>0.416</b>	0.0047	-0.322	0.024	<b>0.423</b>	0.0042
Biomass mean size	-0.184	0.134	<b>0.602</b>	<0.0001	0.280	0.044
SOUR <sup>c</sup>	0.139	0.209	<b>-0.828</b>	<0.0001	0.182	0.144

<sup>a</sup> SVI, sludge volume index; <sup>b</sup>MCRT, mean cell retention time; <sup>c</sup>SOUR, specific oxygen utilization rate

Correlation coefficients with significant coefficients *P* < 0.01 were printed in bold

existed discrepancy in time between the emergence of maturation phase in terms of aerobic granulation and the appearance of stable microbial community. For the appearance of stable microbial community, the reactor needed to be operated for further two months after entering into the maturation phase of granulation. However, the appearance of stable microbial community corresponded to the beginning of relatively stable biomass concentrations and biomass activity in Phase I.

While the initial change in bacterial community could be attributed naturally to the adaptation of the seeded activated sludge to new operational conditions in the reactor, the stable communities established with further reactor operation might be ascertained through incorporating other factors specific to the reactor system. Stable microbial communities have been found in engineered biofilm reactors under constant condition [5, 12]. Compared to suspension microbial communities, biofilm microorganisms are tolerant of fluctuations in environmental conditions and resilient to minor perturbations as the physical habitat provides some buffering of environmental fluctuations [3, 21]. Aerobic granules can be regarded as special biofilms without carrier, and the physical structure of aerobic granules might help maintain the stable microbial community under constant conditions.

The high resilience of microbial community in aerobic granules might also relate to the effect of operational selection pressures, which could lead to the stable microbial community more resistant to environmental disturbance [19]. Aerobic granulation is caused under strong hydraulic selection pressure which was maintained through employment of a very short settling and discharge time strategy to select and retain compact microbial aggregates and wash out light and dispersed particles for aerobic granulation [18]. As a result, distinct microbes well adapted to this repetitive hydraulic selection were favorably selected and proliferated. The reactor was operated in sequencing batch mode. One unique feature of SBRs different from continuous systems is that the cells in SBRs are exposed to alternating feast and famine conditions. A high phenol concentration in the initial period of each cycle was toxic to most bacteria, and also played roles in selection of microbial community.

Recently, it was found that biological processes might be linked with some specific dominant microbial populations [11, 20, 28]. Therefore, some dominant bacterial species were assumed to play an important role in maintaining the physical structure of aerobic granules and degrading pollutants [15, 17]. Two DGGE bands B04 and B09 for the biomass at the end of the experiment belonged to the genera *Zoogloea* and *Comamonas*, respectively. Strains in the two genera have long been considered the typical activated sludge bacterium responsible for the

formation of activated sludge flocs [24], and might also make contribution to the structure of aerobic granules.

In bioreactors, there existed associations between particular environmental variables and certain populations [13]. In the present study, biomass concentration and biomass loading were found to be significantly related to PC 1 from the PCA of the DGGE profiles, which explained a major portion of the variance of bacterial communities. The phenol toxicity exerted on the microbial community is inversely correlated to biomass concentration. Then, bioreactors capable of retaining high biomass concentrations possess strong ability to buffer and reduce the toxicity of this compound. Although a shock loading of 6 g phenol L<sup>-1</sup> day<sup>-1</sup> caused the strong inhibition on biomass activity, the aerobic granules-based bioreactor still could completely remove phenol during this 10-day period (Fig. 2). Besides serving a function in protecting microorganism within the granules against high phenol concentrations [26], granule structure allows retention of high biomass concentration in the reactor to improve the degradation capacity and operational stability of aerobic granule-based systems.

Accompanied with the shock loading, biomass concentrations and granule properties varied dramatically. After the shock loading, the physical structures and activity of aerobic granules were not able to return to the state prior to the disturbance. Compared to aerobic granules with small sizes and high activity prior to the disturbance, aerobic granules after disturbance were characterized with large sizes and low specific activity, although operational conditions in the Phase III were same as those in Phase I. The low activities of granules at the end of Phase III might be related to large sizes of granules as substrate and oxygen diffusion limitation can pose a serious problem in big granules, although the granular structure serves as important function in protecting microorganism within the granules against high phenol concentrations. Therefore, the capacity of aerobic granules-based bioreactors would be improved if the granule size could be controlled at a level so that the granules consist entirely of actively biodegrading cells. However, the granule size was affected by many parameters beyond operational conditions. During the shock loading, small granules with poor settleability might be easily washed out and the remaining biomass could then develop into bigger granules over time. After the shock loading, those granules were broken into small and big aggregates with reactor operation. The newly formed granules from big aggregates could then grow to become bigger mature granules [16]. Therefore, the granules with large sizes could continuously exist in Phase III. In addition, the correlation analysis showed that both the mean size and activity of phenol-degrading aerobic granules were related significantly to PC 2 from the PCA of the



DGGE profiles (Table 2). As the PC 2 only explained a small portion of the variance, caution is needed to interpret the coupling between overall bacterial community and mean size. Application of recently developed genomics tools with higher resolution could obtain quantitative information about not only phylogenetic diversity but functional diversity of microbial community within aerobic granules, and then might lead to deep understanding of the effect of microbial community on the physical structure of aerobic granules.

### Supporting Information Available

Sequence similarities to closest relatives and phylogenetic affiliations of DNA recovered from DGGE gel, Photographs of biomass in the reactor, UPGMA analysis of DGGE fingerprints of 16S rDNA gene fragments.

**Acknowledgements** H. L. Jiang was supported financially by Singapore Millennium Foundation and National Natural Science Foundation of China (40971279). Z. W. Zhao was supported by NSF of Jiangsu province, China (BK2009264).

### References

- Adav SS, Lee DJ, Ren NQ (2007) Biodegradation of pyridine using aerobic granules in the presence of phenol. *Water Res* 41:2903–2910
- Adav SS, Lee DJ, Lai JY (2009) Functional consortium from aerobic granules under high organic loading rates. *Bioresour Technol* 100:3465–3470
- Araya R, Tani K, Takagi T, Yamaguchi N, Nasu M (2003) Bacterial activity and community composition in stream water and biofilm from an urban river determined by fluorescent in situ hybridization and DGGE analysis. *FEMS Microbiol Ecol* 43:111–119
- Beun JJ, Hendriks A, van Loosdrecht MCM, Morgenroth E, Wilderer PA, Heijnen JJ (1999) Aerobic granulation in a sequencing batch reactor. *Water Res* 33:2283–2290
- Carvalho MF, Jorge RF, Pacheco CC, de Marco P, Henriques IS, Correia A, Castro PML (2006) Long-term performance and microbial dynamics of an up-flow fixed bed reactor established for the biodegradation of fluorobenzene. *Appl Microbiol Biotechnol* 71:555–562
- Cassidy DP, Belia E (2005) Nitrogen and phosphorus removal from an abattoir wastewater in a SBR with aerobic granular sludge. *Water Res* 39:4817–4823
- Chen Y, Jiang W, Liang DT, Tay JH (2008) Biodegradation and kinetics of aerobic granules under high organic loading rates in sequencing batch reactor. *Appl Microbiol Biotechnol* 79:301–308
- de Kreuk M, Heijnen JJ, van Loosdrecht MCM (2005) Simultaneous COD, nitrogen, and phosphate removal by aerobic granular sludge. *Biotechnol Bioengin* 90:761–769
- Eichner CA, Erb RW, Timmis KN, Wagner-Dobler I (1999) Thermal gradient gel electrophoresis analysis of bioprotection from pollutant shocks in the activated sludge microbial community. *Appl Environ Microbiol* 65:102–109
- Fromin N, Hamelin J, Tarnawski S, Roesti D, Jourdain-Miserez K, Forestier N, Teyssier-Cuvelles S, Gillet F, Aragno M, Rossi P (2002) Statistical analysis of denaturing gel electrophoresis (DGE) fingerprinting patterns. *Environ Microbiol* 4:634–643
- Futamata H, Nagano Y, Watanabe K, Hiraishi A (2005) Unique kinetic properties of phenol-degrading *Variovovax* strains responsible for efficient trichloroethylene degrading in a chemostat enrichment culture. *Appl Environ Microbiol* 65:3697–3704
- Gentile M, Yan T, Tiquia SM, Fields MW, Nyman J, Zhou J, Criddle CS (2006) Stability in a denitrifying fluidized bed reactor. *Microb Ecol* 52:311–321
- Hwang C, Wu W, Gentry TJ, Carley J, Corbin GA, Carroll SL, Watson DB, Jardine PM, Zhou J, Criddle CS, Fields MW (2009) Bacterial community succession during in situ uranium bioremediation: spatial similarities along controlled flow paths. *ISME J* 3:47–64
- Jiang HJ, Tay JH, Tay STL (2002) Aggregation of immobilized activated sludge cells into aerobically grown microbial granules for the aerobic biodegradation of phenol. *Lett Appl Microbiol* 35:439–445
- Jiang HJ, Tay JH, Maszenan AM, Tay STL (2004) Bacterial diversity and function of aerobic granules engineered in a sequencing batch reactor for phenol degradation. *Appl Environ Microbiol* 70:6767–6775
- Lemaire R, Webb RI, Yuan Z (2008) Micro-scale observations of the structure of aerobic microbial granules used for the treatment of nutrient-rich industrial wastewater. *ISME J* 2:528–541
- Li AJ, Yang SF, Li XY, Gu JD (2008) Microbial population dynamics during aerobic sludge granulation at different organic loading rates. *Water Res* 42:3552–3560
- Liu Y, Wang ZW, Qin L, Liu YQ, Tay JH (2005) Selection pressure-driven aerobic granulation in a sequencing batch reactor. *Appl Microbiol Biotechnol* 67:26–32
- Lozada M, Figuerola ELM, Itria RF, Erijman L (2006) Replicability of dominant bacterial populations after long-term surfactant-enrichment in lab-scale activated sludge. *Environ Microbiol* 8:625–638
- Manefield M, Whiteley AS, Griffiths RI, Bailey MJ (2002) RNA stable isotope probing, a novel means of linking microbial community function to Phylogeny. *Appl Environ Microbiol* 68:5367–5373
- Moss JA, Nocker A, Lepo JE, Snyder RA (2006) Stability and change in estuarine biofilm bacterial community diversity. *Appl Environ Microbiol* 72:5679–5688
- Muyzer G, Dewaal EC, Uitterlinden AG (1993) Profiling of complex microbial-populations by denaturing gradient gel-electrophoresis analysis of polymerase chain reaction-amplified genes-coding for 16s ribosomal-RNA. *Appl Environ Microbiol* 59:695–700
- Nanchaiaiah YV, Schwarzenbeck N, Mohan TVK, Narasimhan SV, Wilderer PA, Venugopalan VP (2006) Biodegradation of nitritotriacetic acid (NTA) and ferric-NTA complex by aerobic microbial granules. *Water Res* 40:1539–1546
- Seviour RJ, Blackall LL (1999) *The microbiology of activated sludge*. Kluwer Academic Publishers, London
- Su KZ, Yu HQ (2005) Formation and characterization of aerobic granules in a sequencing batch reactor treating soybean-processing wastewater. *Environ Sci Technol* 39:2818–2827
- Tay JH, Jiang HL, Tay STL (2004) High-rate biodegradation of phenol by aerobically grown microbial granules. *J Environ Engin-ASCE* 130:1415–1423
- Tay STL, Zhuang WQ, Tay JH (2005) Start-up, microbial community analysis and formation of aerobic granules in a tert-butyl alcohol degrading sequencing batch reactor. *Environ Sci Technol* 39:5774–5780

28. Watanabe K, Teramoto M, Harayama S (1999) An outbreak of nonflocculating catabolic populations caused the breakdown of a phenol-digesting activated-sludge process. *Appl Environ Microbiol* 65:2813–2819
29. Yi S, Zhuang WQ, Wu B, Tay STL, Tay JH (2006) Biodegradation of p-nitrophenol by aerobic granules in a sequencing batch reactor. *Environ Sci Technol* 40:2396–2401